

Temperature dependence of intersubband transitions in InAs/AlSb quantum wells

D. C. Larrabee, G. A. Khodaparast, and J. Kono^{a)}

Department of Electrical and Computer Engineering, Rice Quantum Institute, and Center for Nanoscale Science and Technology, Rice University, Houston, Texas 77005

K. Ueda, Y. Nakajima, M. Nakai, S. Sasa, and M. Inoue

New Materials Research Center, Osaka Institute of Technology, Osaka 535-8585, Japan

K. I. Kolokolov, J. Li, and C. Z. Ning

Center for Nanotechnology, NASA Ames Research Center, Moffett Field, California 94035

(Received 29 April 2003; accepted 17 September 2003)

We have carried out a systematic temperature-dependent study of intersubband absorption in InAs/AlSb quantum wells from 5 to 10 nm well width. The resonance energy redshifts with increasing temperature from 10 to 300 K, and the amount of redshift increases with decreasing well width. We have modeled the transitions using eight-band $\mathbf{k}\cdot\mathbf{p}$ theory combined with semiconductor Bloch equations, including the main many-body effects. Temperature is incorporated via band filling and nonparabolicity, and good agreement with experiment is achieved for the temperature dependence of the resonance. © 2003 American Institute of Physics. [DOI: 10.1063/1.1626264]

The family of semiconductors with a lattice constant around 6.1 Å—InAs, GaSb, and AlSb—are a promising system for applications in heterostructure devices such as long-wavelength detectors¹ and lasers.² Interband infrared applications rely on the small bandgap of InAs and the possibility of broken-gap type-II band alignment between InAs and GaSb. On the other hand, intraband applications can take advantage of the enormous conduction band offset in InAs/AlSb heterostructures—as large as 2 eV. The resulting deep well allows intersubband transitions (ISBTs) ranging in energy from the near-infrared (NIR) to the far-infrared. One application of deep wells that was recently proposed is an intersubband terahertz laser pumped by a compact NIR diode laser.³ In order to realize such a source, it is necessary first to understand thoroughly intersubband absorption in this material system.

Previous experimental studies of ISBTs in InAs/AlSb quantum wells (QWs) have focused on a variety of aspects. For example, Warburton *et al.* have observed the ISBT in doped InAs/AlSb QWs from 6 to 18 nm well width, and concluded that interface roughness scattering dominates the linewidth of the resonance.⁴ They have also studied the temperature dependence of an 18 nm QW with two populated subbands, in which case Landau damping becomes an important scattering mechanism. Prevot *et al.* have studied 6.5 to 8.6 nm undoped QWs at low temperature, both with and without interband optical pumping.⁵ Recently, Ohtani *et al.* have observed ISBTs at room temperature in doped QWs from 5.4 nm to as narrow as 2.7 nm.⁶

In this letter, we present detailed temperature-dependent measurements of the ISBT in 5 to 10 nm undoped InAs/AlSb QWs. We observe a redshift of the ISBT with increasing temperature. The amount of redshift increases with decreasing

well width, from 6.2 meV for the 10 nm sample to 12.0 meV for the 5 nm sample. Similar, but much smaller, redshifts have been reported for ISBTs in GaAs/AlGaSb QWs.^{7,8} A simple theory, taking into account only the temperature dependence of the effective mass and band offset, would predict a blueshift of the ISBT energy with increasing temperature. To explain these results correctly, we have developed a theoretical model based on the density matrix formalism. It incorporates all the major many-body effects via the semiconductor Bloch equations and nonparabolic subband dispersions via eight-band $\mathbf{k}\cdot\mathbf{p}$ calculations. Our model gives good agreement with the observed temperature dependence of the ISBT energy.

The samples were grown by molecular-beam epitaxy on a semi-insulating GaAs substrate. The buffer structure consisted of GaAs (300 nm)/AlAs (10 nm)/AlSb (100 nm)/GaSb (300 nm)/AlSb (1000 nm)/[AlSb/GaSb (6 nm/6 nm)] \times 15/AlGaSb (200 nm). The active region consisted of 20 periods of InAs/AlSb ($x/10$ nm), where $x=5$ to 10 nm, and it was capped by 10 nm of GaSb. The QW interfaces were grown InSb-like,⁹ and the wells were under tensile strain. The samples were not intentionally doped, but had a total electron density of 1.8×10^{12} to 6.9×10^{13} cm⁻² at 77 K. The most likely sources of electrons in these wells are bulk¹⁰ and interface¹¹ donors and Fermi level pinning at the surface of the GaSb cap layer.¹² We attribute the large variation in total electron density to variation in the density of bulk donors. In this work, we compare samples with roughly the same total electron density, around 1×10^{13} cm⁻² (see Table I), and a per-well density of about 1×10^{12} cm⁻². For this per-well density, only the lowest subband is populated.

The ISBT was measured with a Fourier-transform infrared spectrometer in a multibounce geometry. The QW surface was coated with 100 nm of gold and the sample edges were polished to 45°. A wire grid polarizer was placed before the sample and the ratio of *p*- and *s*-polarized transmission

^{a)}Author to whom correspondence should be addressed; electronic mail: kono@rice.edu

TABLE I. Samples considered in this letter. The density given is the total density. All samples contain 20 periods of InAs/AlSb QWs.

Sample	Well width (nm)	300 K density (cm ⁻²)	77 K density (cm ⁻²)
A	10	5.47×10^{12}	2.56×10^{12}
B	8.4	1.46×10^{13}	1.20×10^{13}
C	7.5	1.83×10^{13}	1.68×10^{13}
D	7	2.63×10^{13}	2.46×10^{13}
E	6.5	1.94×10^{13}	1.75×10^{13}
F	6	1.62×10^{13}	1.58×10^{13}
G	5	1.61×10^{13}	1.36×10^{13}

(ISBT active and inactive) was taken. The background was the p/s ratio with no sample. The absorption coefficient of the sample α was calculated as $\alpha = [-\ln(T) + R]/L$, where T is the p/s transmission ratio of the sample divided by the p/s transmission ratio with no sample, R is a sample-dependent constant chosen to make α equal zero away from the absorption, and L is the total length of well material that the infrared beam passes through.

Intersubband absorption spectra for samples A–G at various temperatures between 10 and 300 K are shown in Fig. 1. The absorption coefficient of the sample α is plotted versus energy. The ISBT energy increases with decreasing well width from 212 meV (5.84 μm) for 10 nm wells to 385 meV (3.22 μm) for 5 nm wells at 10 K. For a given well width, the ISBT peak position redshifts with increasing temperature. The amount of redshift increases with decreasing well width from 6.2 meV for 10 nm to 12.0 meV for 5 nm, as shown in Fig. 2(a). The ISBT linewidth has a weak temperature dependence, increasing from 10 to 300 K by a factor of less than 2, as shown in Fig. 2(b). The low-temperature linewidths are relatively small, ranging from 11 to 23 meV (2.8 to 5.8 THz), indicating that the interface type and smoothness are well controlled. The ISBT linewidth does not vary systematically with well width.

Modeling of ISBTs is complicated by the strong influ-

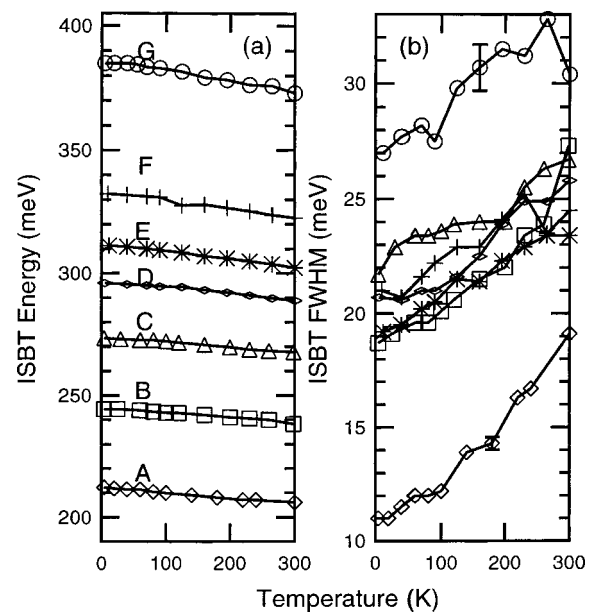


FIG. 2. Temperature dependence of intersubband absorption (a) peak energy and (b) width at half-maximum for seven InAs/AlSb QW samples with well widths from 10 to 5 nm (corresponding to samples A–G in Fig. 1).

ence of many-body effects:¹³ the self-energy or exchange correction, the depolarization shift, and the vertex or excitonic correction. InAs/AlSb systems are particularly interesting due to the interplay between these many-body effects and the strong nonparabolicity of the InAs conduction band.^{14,15} For example, our calculations show that, for a 10 nm well, the self-energy and depolarization correction both cause a significant blueshift and broadening of the single-particle spectrum. However, the vertex correction causes the absorption to redshift, narrow, and increase in intensity, which nearly cancels out the other effects.

Our model is based on an eight-band $\mathbf{k}\cdot\mathbf{p}$ theory, and the many-body effects on the absorption are incorporated through the semiconductor Bloch equations. A detailed de-

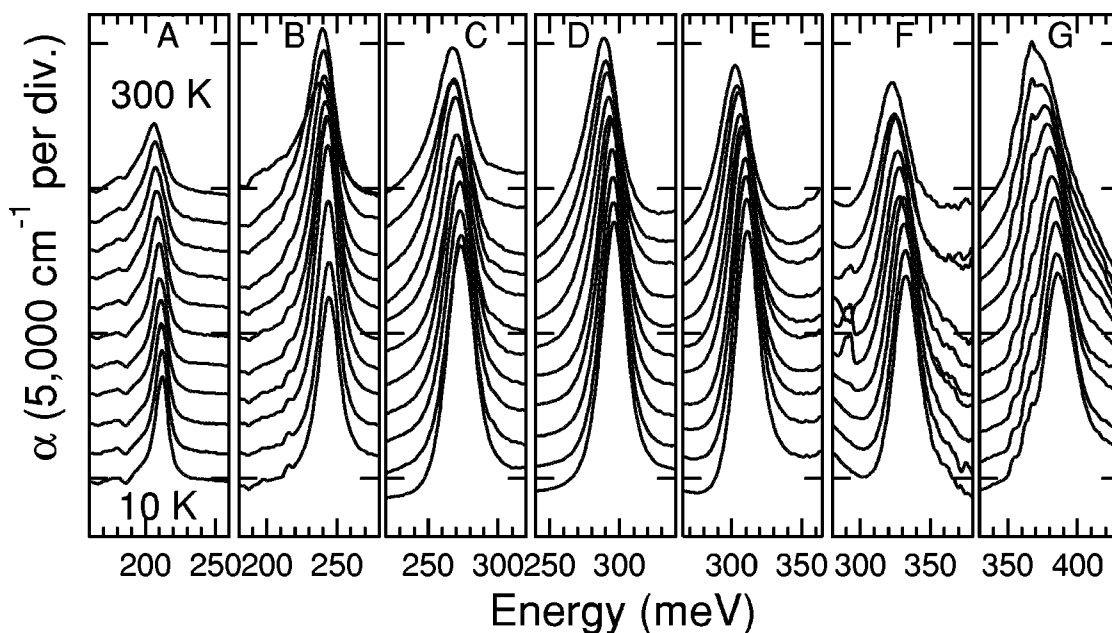


FIG. 1. Intersubband absorption spectra of InAs/AlSb QWs. The absorption coefficient is plotted as a function of energy from 10 to 300 K with a temperature interval of ~ 30 K.

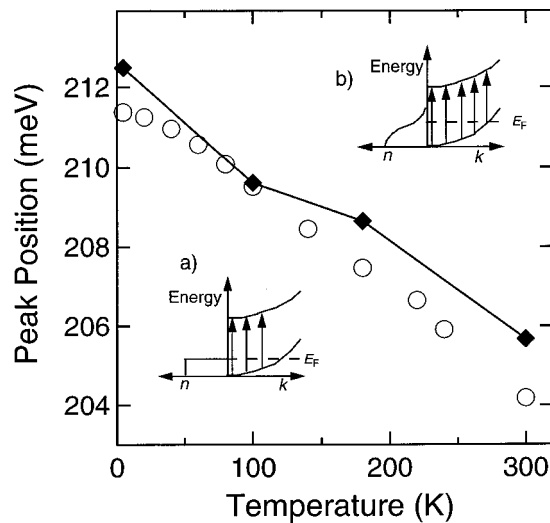


FIG. 3. The measured (circles) and calculated (squares) intersubband absorption peak energies as a function of temperature for sample A. The lines are guides for the eye. The insets show the carrier distribution (n) and subband dispersions (k) with possible single-particle absorption (arrows) at (a) low and (b) high temperature, illustrating the redshift of the intersubband resonance with increasing temperature.

scription of the model will be given in a future publication.¹⁶ We first calculate the band structure using an eight-band $\mathbf{k}\cdot\mathbf{p}$ theory, which includes the charge profile via the Hartree potential as well as strain effects. Next, the interaction with light is computed. The Hamiltonian is written in terms of creation and annihilation operators, from which the population and polarization variables can be derived. They are used to find an expression for the linear susceptibility, the imaginary part of which is the absorption. The obtained linear susceptibility includes all the major many-body effects as well as LO phonon and interface roughness scattering.

We have simulated the ISBT as a function of temperature for a 10 nm well, as shown in Fig. 3. The redshift of the peak is mainly due to band filling coupled with strong nonparabolicity. Increasing temperature leads to population of large wave-vector states. Strong nonparabolicity leads to significant decrease in the transition energy with increasing electron wave vector. The combination therefore causes a reduction of the transition energy with increasing temperature. This effect also explains why a smaller redshift (~ 3 meV) was observed for GaAs QWs:^{7,8} because of their smaller nonparabolicity. The eight-band $\mathbf{k}\cdot\mathbf{p}$ band-structure calculation takes the nonparabolicity into account accurately, leading to a good agreement with experiment. In this simulation we kept the density constant and included the decrease in the effective mass with increasing temperature,¹⁷ which causes a small blueshift.

In conclusion, we have measured the temperature depen-

dence of the intersubband absorption in undoped InAs/AlSb QWs. The absorption shows a strong redshift with increasing temperature. In addition, we have modeled the intersubband absorption using an eight-band $\mathbf{k}\cdot\mathbf{p}$ band structure and the semiconductor Bloch equations, which include the major many-body effects on an equal footing. The redshift is incorporated via band filling and nonparabolicity. These results are promising for the development of optically pumped intersubband far-infrared emitters.

We gratefully acknowledge support from DARPA/AFOSR F49620-01-1-0543 (ABCS), NASA-NCIBSRP, the Robert A. Welch Foundation, NSF DMR-0134058 (CAREER), and NSF INT-0221704. We are grateful to J. Tang and M. Liang for sample preparation, S. M. Crankshaw for transport measurements, and A. J. Rimbarg for the use of his evaporator.

- ¹C. Mailhot and D. L. Smith, *J. Vac. Sci. Technol. A* **7**, 445 (1989); H. Mohseni, E. Michel, J. Sandoen, M. Razeghi, W. Mitchel, and G. Brown, *Appl. Phys. Lett.* **71**, 1403 (1997).
- ²K. Ohtani and H. Ohno, *Appl. Phys. Lett.* **82**, 1003 (2003); J. L. Bradshaw, R. Q. Yang, J. D. Bruno, J. T. Pham, and D. E. Wortman, *ibid.* **75**, 2362 (1999); W. W. Bewley, C. L. Felix, I. Vurgaftman, D. W. Stokes, E. H. Aifer, L. J. Olafsen, J. R. Meyer, M. J. Yang, B. V. Shanabrook, H. Lee, and R. U. Martinelli, *ibid.* **74**, 1075 (1999); M. E. Flatte, T. C. Hasenberg, J. T. Olesberg, S. A. Anson, T. F. Boggess, C. Yan, and D. L. McDaniel, *ibid.* **71**, 3764 (1997); see also, *Antimonide-Related Strained-Layer Heterostructures*, edited by M. O. Manasreh (OPA, Amsterdam, 1997).
- ³A. Liu and C. Z. Ning, *Appl. Phys. Lett.* **76**, 1984 (2000).
- ⁴R. J. Warburton, K. Weillhammer, C. Jabs, J. P. Kotthaus, M. Thomas, and H. Kroemer, *Physica E (Amsterdam)* **7**, 191 (2000).
- ⁵I. Prevot, B. Vinter, F. H. Julien, F. Fossard, and X. Marcadet, *Phys. Rev. B* **64**, 195318 (2001).
- ⁶K. Ohtani, N. Matsumoto, H. Sakuma, and H. Ohno, *Appl. Phys. Lett.* **82**, 37 (2003).
- ⁷B. C. Covington, C. C. Lee, B. H. Hu, H. F. Taylor, and D. C. Streit, *Appl. Phys. Lett.* **54**, 2145 (1989).
- ⁸M. O. Manasreh, F. Szmulowicz, D. W. Fischer, K. R. Evans, and C. E. Stutz, *Appl. Phys. Lett.* **57**, 1790 (1990).
- ⁹M. Yano, M. Okuizumi, Y. Iwai, and M. Inoue, *J. Appl. Phys.* **74**, 7472 (1993).
- ¹⁰S. Ideshita, A. Furukawa, Y. Mochizuki, and M. Mizuta, *Appl. Phys. Lett.* **60**, 2549 (1992).
- ¹¹G. Tuttle, H. Kroemer, and J. H. English, *J. Appl. Phys.* **67**, 3032 (1990); H. Kroemer, C. Nguyen, and B. Brar, *J. Vac. Sci. Technol. B* **10**, 1769 (1992).
- ¹²C. Nguyen, B. Brar, H. Kroemer, and J. H. English, *Appl. Phys. Lett.* **60**, 1854 (1992).
- ¹³See, for example, T. Ando, *Solid State Commun.* **21**, 133 (1977); T. Ando, *Z. Phys. B* **26**, 263 (1977); T. Ando, A. B. Fowler, and F. Stern, *Rev. Mod. Phys.* **54**, 437 (1982).
- ¹⁴R. J. Warburton, C. Gauer, A. Wixforth, J. P. Kotthaus, B. Brar, and H. Kroemer, *Phys. Rev. B* **53**, 7903 (1996).
- ¹⁵D. E. Nikonov, A. Imamoglu, L. V. Butov, and H. Schmidt, *Phys. Rev. Lett.* **79**, 4633 (1997).
- ¹⁶For preliminary results, see J. Li, K. I. Kolokolov, C. Z. Ning, D. C. Larrabee, G. A. Khodaparast, J. Kono, K. Ueda, Y. Nakajima, S. Sasa, and M. Inoue, *Mater. Res. Soc. Symp. Proc.* **744**, M9.2.1 (2003).
- ¹⁷R. A. Stradling and R. A. Wood, *J. Phys. C* **3**, L94 (1970).